SPACE TELESCOPE SCIENCE INSTITUTE
Operated for NASA by AURA

Instrument Science Report ACS 2003-05

ACS Background Light vs. Bright Earth Limb Angle

J. Biretta, D. Van Orsow, W. Sparks, M. Reinhart, and A. Vick
June 23, 2003

ABSTRACT

We present results of the ACS Bright Earth Limb calibration program 9660. The background contributed by scattered Earth light is found to be relatively constant for bright Earth limb angles in the range 25 to 30 degrees, but at smaller angles the background increases exponentially and reaches values 40 (WFC) and 100 (HRC) times higher by limb angles of 14 degrees. This general trend is similar to that previously reported for STIS, though the rate of increase at small angles is even more rapid for ACS. Besides the increased background level, there are also significant flat field artifacts in the background which would compromise observations of faint targets. Based on these results, it appears unlikely that much benefit could be gained by decreasing the so-called "bright Earth avoidance" angle for ACS observations.

Introduction

In an effort to minimize the background light in HST images, observations are normally scheduled only when the telescope will be pointed more than a certain angle from the bright Earth limb. This angle, called the Bright Earth Avoidance angle, is currently 20° for most HST observations, including ACS. Herein we explore the dependence of the background light on bright Earth limb angle for ACS, and consider whether a change (decrease) in the avoidance angle appears desirable. Decreasing the avoidance angle could potentially increase the amount of available HST observing time. For targets near the celestial equator, the potential increase is quite modest -- each 1° decrease in the avoidance angle only increases the observing time by about 15 sec. per orbit. However, for

targets near the HST orbit poles (i.e. near the Continuous Viewing Zone or CVZ), the increase in observing time could be many minutes per orbit.

Observations

A relatively empty field in the north CVZ was selected such that HST's pointing would graze the bright Earth limb while observing the field. Four single-orbit visits were carried out. During each visit an uninterrupted sequence of images were obtained without CR-SPLITS. Table 1 lists the cameras and filters used. During the WFC observations parallel data were also obtained with the STIS CCD.

Table 1. Summary of Observations in Program 9660

Visit	Camera	Filter	Exposure Time	Notes
1	WFC	F606W	350s	8 exposures
2	WFC	F850LP	350s	8 exposures
3	HRC	F606W	120s	28 exposures
4	HRC	F250W	240s	18 exposures

Background Light vs. Bright Earth Limb Angle

Table 2 lists the circumstances and measured background light for each ACS exposure. For each visit the first line of entries gives the visit number, the camera, filter, exposure time, and observation date. Each subsequent line gives the details of each individual exposure. The Earth limb angles, defined as the angle between the HST pointing and the nearest Earth limb, are given at the start and end of the exposure, as well as whether the limb was sunlit (bright) or dark. The background light in each image was measured using the IMSTAT "midpt" (median) statistic applied to the entire image excluding a 100 pixel border around the edges.[1] Pixels outside the range -100 to 1000 DN were also excluded.[2]

1. For the WFC only CCD #2 was measured.
2. For the HRC F250W a smaller range of -20 to 20 DN was used since there were very few counts.

These measures should provide adequate rejection of cosmic rays and other anomalous pixels. The resulting background counts per pixel are given in the last column.

Table 2. Results: Earth Limb Angles and Measured Background Counts

Visit	Camera	Filter	Exp. Time (s)	Day		
Image	Start Time	Start		End		Median Backgrnd Counts per Pixel
		Earth Limb Bright?	Earth Limb Angle (deg.)	Earth Limb Bright?	Earth Limb Angle (deg.)	
Visit 1	WFC	F606W	350s	2002:364		
j8l501aaq_flt.fits[1]	01:16:37	N	30.47	N	27.69	22.8
j8l501agq_flt.fits[1]	01:24:43	N	26.41	Y	22.91	23.9
j8l501anq_flt.fits[1]	01:34:48	Y	20.37	Y	17.30	115.0
j8l501auq_flt.fits[1]	01:44:53	Y	15.59	Y	14.25	549.4
j8l501b1q_flt.fits[1]	01:54:58	Y	14.10	Y	15.08	853.9
j8l501b8q_flt.fits[1]	02:05:03	Y	16.57	Y	19.43	94.6
j8l501bfq_flt.fits[1]	02:15:08	Y	21.90	Y	25.43	29.1
j8l501bmq_flt.fits[1]	02:25:13	N	27.85	N	30.60	21.8
Visit 2	WFC	F805LP	350s	2002:364		
j8l502buq_flt.fits[1]	02:52:31	N	30.46	N	27.68	6.5
j8l502c0q_flt.fits[1]	03:00:37	N	26.40	Y	22.90	8.3
j8l502c7q_flt.fits[1]	03:10:42	Y	20.37	Y	17.30	53.0
j8l502ceq_flt.fits[1]	03:20:47	Y	15.60	Y	14.26	205.7
j8l502clq_flt.fits[1]	03:30:52	Y	14.12	Y	15.09	241.
j8l502csq_flt.fits[1]	03:40:57	Y	16.58	Y	19.44	71.7
j8l502czq_flt.fits[1]	03:51:02	Y	21.91	Y	25.44	11.7
j8l502d6q_flt.fits[1]	04:01:07	N	27.86	N	30.59	6.4
Visit 3	HRC	F606W	120s	2002:364		
j8l503e3q_flt.fits[1]	04:27:13	N	31.10	N	30.33	1.09
j8l503e4q_flt.fits[1]	04:30:04	N	29.97	N	29.05	1.15
j8l503e5q_flt.fits[1]	04:32:55	N	28.62	N	27.57	1.20
j8l503e6q_flt.fits[1]	04:35:46	N	27.10	N	25.94	0.99
j8l503e7q_flt.fits[1]	04:38:37	Y	25.44	Y	24.23	1.25
j8l503e9q_flt.fits[1]	04:41:28	Y	23.71	Y	22.50	1.63

Table 2. Results: Earth Limb Angles and Measured Background Counts

Visit	Camera	Filter	Exp. Time (s)	Day		
Image	Start Time	Start		End		Median Backgrnd Counts per Pixel
		Earth Limb Bright?	Earth Limb Angle (deg.)	Earth Limb Bright?	Earth Limb Angle (deg.)	
j8l503eaq_flt.fits[1]	04:44:19	Y	21.98	Y	20.79	2.86
j8l503ebq_flt.fits[1]	04:47:10	Y	20.30	Y	19.17	4.5
j8l503ecq_flt.fits[1]	04:50:01	Y	18.73	Y	17.70	7.6
j8l503eeq_flt.fits[1]	04:52:52	Y	17.30	Y	16.43	12.6
j8l503efq_flt.fits[1]	04:55:43	Y	16.09	Y	15.39	14.8
j8l503egq_flt.fits[1]	04:58:34	Y	15.14	Y	14.64	37.4
j8l503ehq_flt.fits[1]	05:01:25	Y	14.47	Y	14.19	83.
j8l503ejq_flt.fits[1]	05:04:16	Y	14.12	Y	14.07	106.
j8l503ekq_flt.fits[1]	05:07:07	Y	14.10	Y	14.27	99.9
j8l503elq_flt.fits[1]	05:09:58	Y	14.40	Y	14.80	59.0
j8l503emq_flt.fits[1]	05:12:49	Y	15.02	Y	15.63	23.5
j8l503enq_flt.fits[1]	05:15:40	Y	15.93	Y	16.72	11.8
j8l503eoq_flt.fits[1]	05:18:31	Y	17.10	Y	18.05	8.2
j8l503epq_flt.fits[1]	05:21:22	Y	18.48	Y	19.56	5.3
j8l503eqq_flt.fits[1]	05:24:13	Y	20.04	Y	21.21	4.01
j8l503erq_flt.fits[1]	05:27:04	Y	21.71	Y	22.92	2.11
j8l503esq_flt.fits[1]	05:29:55	Y	23.44	Y	24.66	1.36
j8l503etq_flt.fits[1]	05:32:46	Y	25.17	N	26.35	0.99
j8l503euq_flt.fits[1]	05:35:37	N	26.84	N	27.94	1.13
j8l503evq_flt.fits[1]	05:38:28	N	28.39	N	29.38	1.23
j8l503ewq_flt.fits[1]	05:41:19	N	29.77	N	30.61	1.05
j8l503exq_flt.fits[1]	05:44:10	N	30.93	N	31.59	0.98
Visit 4	HRC	F250W	240s	2002:364		
j8l504f5q_flt.fits[1]	06:03:43	N	31.14	N	29.49	-0.16
j8l504f6q_flt.fits[1]	06:08:29	N	29.13	N	27.01	-0.25
j8l504f7q_flt.fits[1]	06:13:17	N	26.55	Y	24.16	0.04
j8l504f8q_flt.fits[1]	06:18:04	Y	23.68	Y	21.26	0.11

Table 2. Results: Earth Limb Angles and Measured Background Counts

Visit	Camera	Filter	Exp. Time (s)	Day		
Image	Start Time	Start		End		Median Backgrnd Counts per Pixel
		Earth Limb Bright?	Earth Limb Angle (deg.)	Earth Limb Bright?	Earth Limb Angle (deg.)	
j8l504f9q_flt.fits[1]	06:22:51	Y	20.79	Y	18.55	-0.08
j8l504faq_flt.fits[1]	06:27:37	Y	18.16	Y	16.32	0.13
j8l504fbq_flt.fits[1]	06:32:25	Y	16.01	Y	14.77	0.38
j8l504fcq_flt.fits[1]	06:37:11	Y	14.60	Y	14.07	0.22
j8l504fdq_flt.fits[1]	06:41:59	Y	14.04	Y	14.29	0.26
j8l504feq_flt.fits[1]	06:46:46	Y	14.42	Y	15.41	0.31
j8l504ffq_flt.fits[1]	06:51:33	Y	15.67	Y	17.30	0.14
j8l504fhq_flt.fits[1]	06:56:20	Y	17.68	Y	19.79	-0.06
j8l504fiq_flt.fits[1]	07:01:07	Y	20.24	Y	22.62	-0.21
j8l504fjq_flt.fits[1]	07:05:54	Y	23.10	Y	25.52	0.05
j8l504fkq_flt.fits[1]	07:10:41	N	25.99	N	28.23	-0.11
j8l504flq_flt.fits[1]	07:15:28	N	28.63	N	30.47	0.04
j8l504fmq_flt.fits[1]	07:20:15	N	30.77	N	32.02	-0.02
j8l504fnq_flt.fits[1]	07:24:22	N	32.05	N	32.68	-0.13
j8l504f5q_flt.fits[1]	06:03:43	N	31.14	N	29.49	-0.16

The results for the WFC are illustrated in Figure 1. The circles indicate F606W data, while the triangles denote F850LP. The large open symbols indicate when the telescope is pointing over the bright Earth limb; the small open symbols indicate pointings over the terminator; and the small filled symbols indicate pointings over the dark Earth limb[1]. Since the background light rises rapidly toward smaller angles, we have used the lesser of the start and end angles for each exposure when plotting the results.

1. While the data in program 9660 do not contain very much data with the bright Earth limb at large angles to the HST pointing (i.e. $>25°$), one can make some inferences. For example, the data points with the dark Earth limb near $27°$ will have the terminator at about $35°$. These data should be roughly equivalent to an observation with the bright Earth limb at $35°$. Hence the dark Earth limb data could effectively be plotted as bright Earth limb points at larger angles.

Figure 1: Background Counts vs. Earth Limb Angle for the WFC.

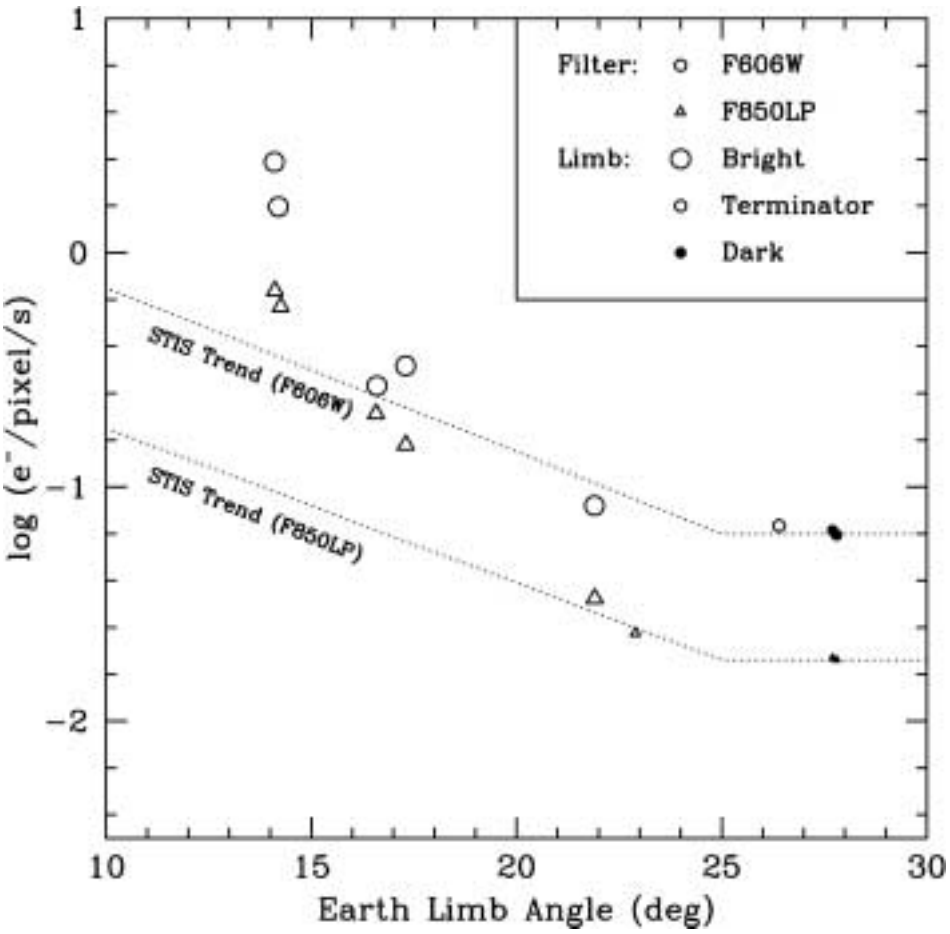

Both filters show relatively constant background counts as the limb angle varies from 30° to ~25°. However, at smaller limb angles the background rises exponentially and increases ~40-fold by 14° . This behavior is similar to that found for STIS CCD data by Shaw, Reinhart, and Wilson (1998, hereinafter SRW98), as illustrated by the two STIS trend lines. They found that the sky background for STIS was approximately constant for bright Earth limb angles down to 25°, but then increased exponentially as $10^{-0.066\alpha}$ where α is the bright Earth limb angle in degrees. The lower line in Figure 2 has been matched to the ACS/WFC F850LP data (triangles) near 25°, and shows that the ACS background rises even more rapidly than for STIS. Similarly, the upper STIS trend line is matched to the

ACS/WFC F606W data (circles) near 25°, and again we find that the background for ACS rises more rapidly than for STIS at small Earth limb angles.[1]

We note our results in units of e^-/sec/pixel can be approximately converted to absolute flux by multiplying by PHOTFLAM, which is 7.9×10^{-20} erg/cm2/Å/e^- and 1.5×10^{-19} erg/cm2/Å/e^-, for F606W and F850LP, respectively. (A more accurate calculation would need to allow for the spectral distribution of the scattered Earth light.) It is also necessary to divide by the square of the plate scale, which is 0.050 arcsec/pixel. Comparison of the absolute background for ACS in F606W at $\alpha = 14^\circ$ shows it is roughly 2.5 times the STIS absolute background found by SRW98 at similar angles.

A more direct comparison with STIS backgrounds is possible since STIS/CCD exposures were taken in parallel with the ACS/WFC observations. We have reduced the STIS data in a manner similar to that for the ACS data. Figure 2 shows the ACS/WFC F606W background plotted as a function of the STIS/CCD background in the parallel data. The dotted line indicates the relationship expected if the ACS background were directly proportional to the STIS background. This appears to be a good approximation at lower background levels corresponding to bright Earth limb angles >16°. But at higher background levels (i.e. smaller bright Earth limb angles) the ACS background is about three times higher than predicted by a simple proportionality to the STIS background.

We can also compare the background count rates in our parallel STIS data with the STIS backgrounds found by SRW98 (their Figure 2). The background in our STIS parallels are well within the range they find, indicating that the Earth brightness during our observations was typical, and in no way anomalous or unexpectedly high.

The cause of the higher background in ACS vs. STIS at small bright Earth limb angles is not entirely clear. One possible cause might be the larger field-of-view of ACS necessarily requires larger aperture stops in the camera, and hence might provide less rejection of light originating outside the normal OTA pupil.

We have also compared our results against the ACS Exposure Time Calculator, and they are in good agreement. The ACS ETC predicts 0.12 e^-/sec/pixel for “bright earthshine” in F606W for the WFC. Interpolating between our data points we predict a maximum background around 0.14 e^-/sec/pixel at the minimum bright Earth angle of 20°. Considering

1. The data points for the dark Earth limb in the range 25° to 30° should be roughly equivalent to data points for the *bright* Earth limb at a somewhat larger angles, as the bright Earth was generally visible to HST, though farther from the pointing direction. In effect, the dark Earth limb data in the range 25° to 30° could be replotted farther to the right at some larger angle corresponding to the effective distance of the bright Earth or terminator. Hence, the general shape of the dependence with angle should remain unchanged if there were more data for the bright Earth limb at large angles.

that the exact background level depends upon the local albedo of the Earth (clouds, soil, water, etc.) this would appear to be an excellent agreement.

Figure 2: ACS/WFC F606W background vs. STIS/CCD parallel data background.

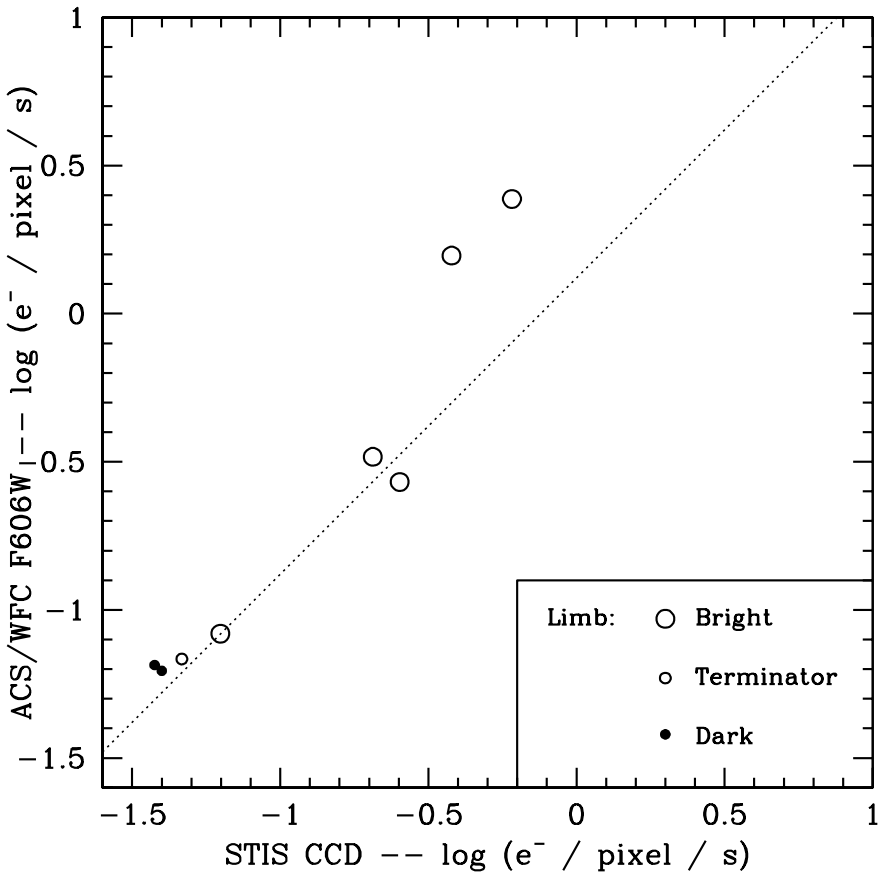

Similar results are obtained for the HRC in F606W (Figure 3), though here the background rises even more rapidly at small angles than for the WFC. The increase seen at 14 degrees is about 40x for the WFC, but is 100x for the HRC.

Figure 3: Background Counts vs. Earth Limb Angle for the HRC in F606W.

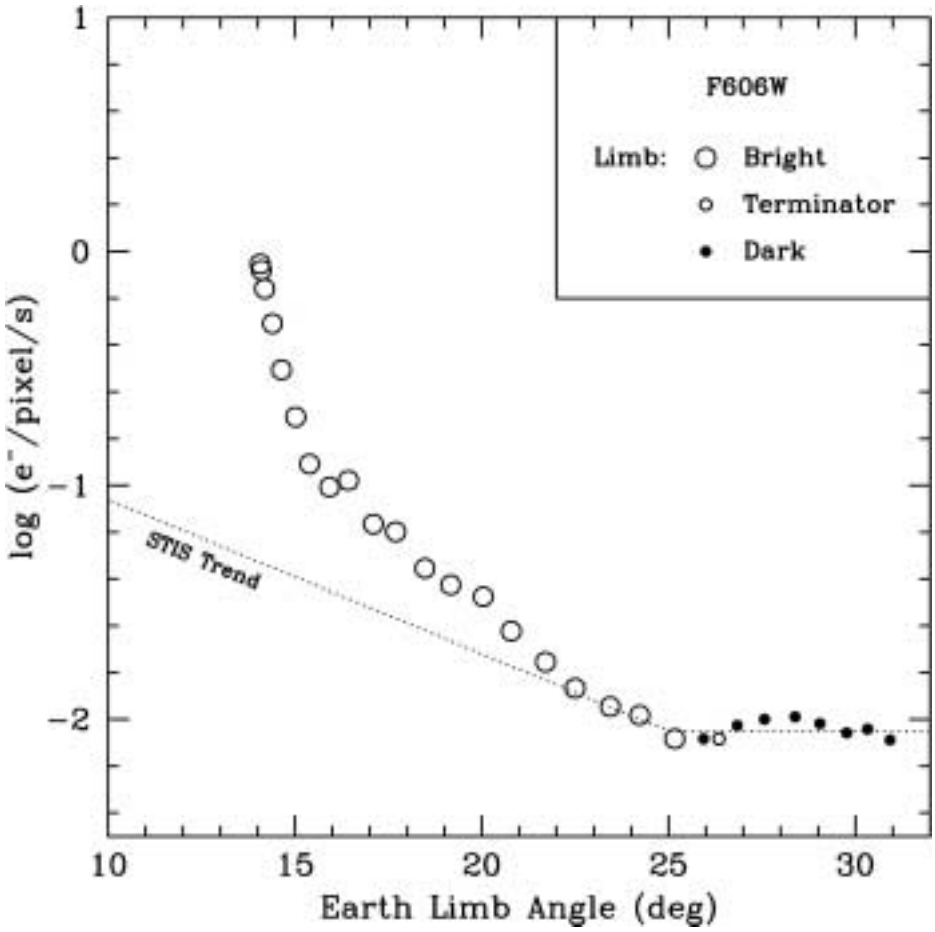

Results for the HRC in F250W are shown in Figure 4. Here the readnoise, etc., dominates the very weak background, but the overall shape of the dependence is probably consistent with the other filters. An interesting aspect of the F250W result, is that it demonstrates that very small Earth limb angles could potentially be used in the ultraviolet with very little image degradation. The same might be true for narrow band filters where the background also would be expected to be very low.

Figure 4: Background Counts vs. Earth Limb Angle for the HRC in F250W.

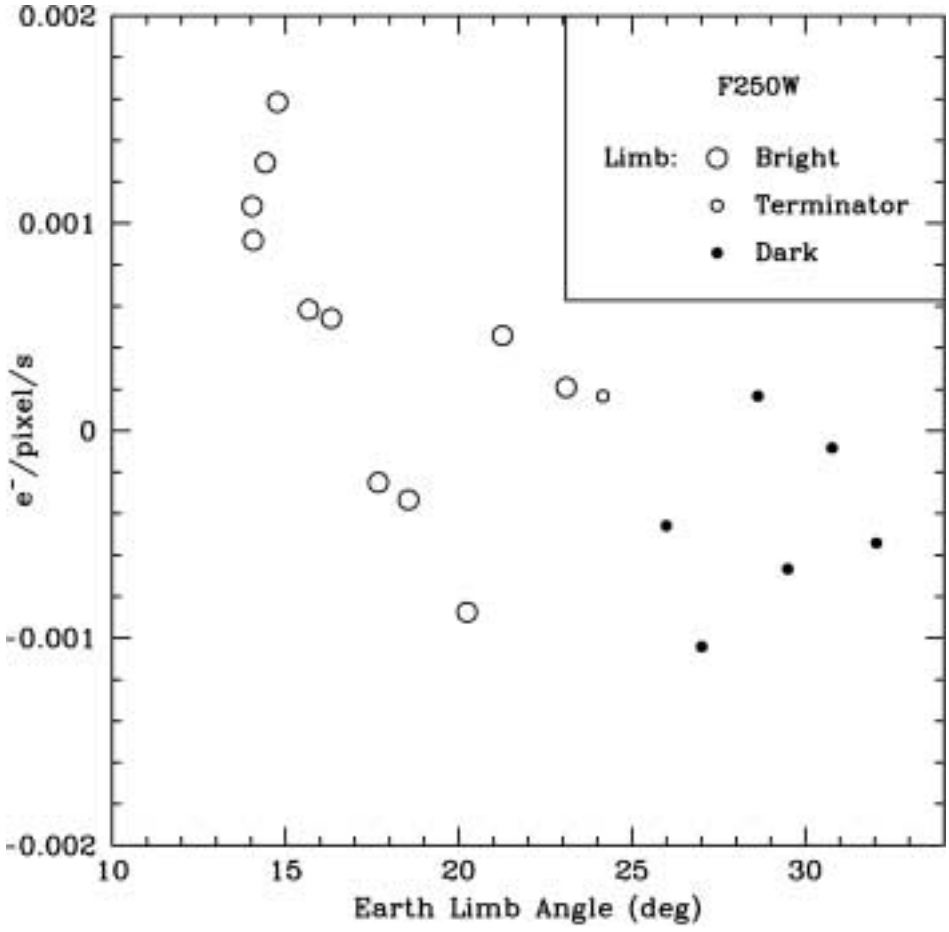

Image Artifacts at Small Earth Limb Angles

Besides the overall elevated background which occurs at small bright Earth limb angles, there are also flat field artifacts in the background which might compromise study of faint targets. These occur because the scattered Earth light is taking a non-standard path through the telescope and camera, and hence flat field artifacts are displaced from their usual positions on the detector. Figure 5 shows a 1500 x 1400 pixel region near the center of WFC2 from image j8l501b1q_flt.fits[1] which had the largest background of the F606W images. There are numerous crescent-shaped artifacts (arrows) which are essentially negative images of the light pattern in the forward OTA; they occur wherever dust particles in the camera block the scattered Earth light. Their size depends upon the location of the dust particle in the optical chain, and the depth of the features depends on the

amount of light blocked by the dust particles. The strongest features in Figure 5 are about 12% deep.

We also examined image j8l501b8q_flt.fits[1] which had a much weaker background (95DN vs. 854DN) and was taken at a larger Earth limb angle (17° vs. 14°). The strongest features there were again about 12% deep, though the artifacts were fewer in number and covered less image area.

In addition to these small-scale features related to the flat fields, there is also a large-scale 18% brightness gradient in the scattered light across the entire WFC field of view.

Image artifacts for the HRC appear to be fewer in number than for the WFC, but are stronger with the strongest reaching ~30%. Any large-scale gradient in background light for the HRC is quite small.

Figure 5: Artifacts in Background Light (WFC F606W). This is a negative display with stars being black, and dark features being white.

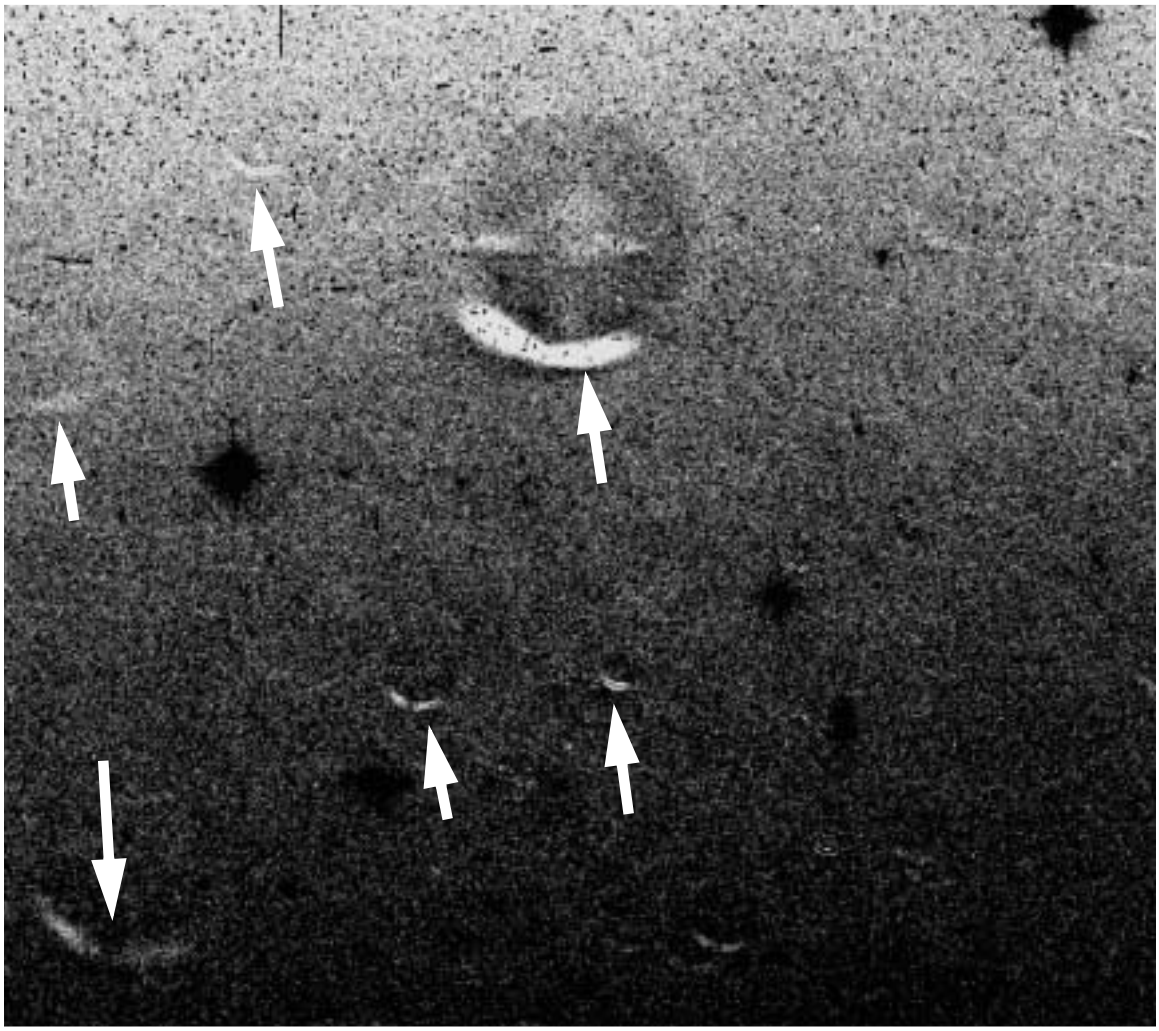

Summary

We find that the background light due to the bright Earth rises very rapidly for bright Earth limb angles below 25°. The increase for a bright Earth limb angle of 14° is about 40x for the WFC, and 100x for the HRC. Comparison to the STIS CCD background shows similar behavior at large angles (>20°), but at smaller angles the ACS background rises more rapidly and reaches levels three (WFC) and ten (HRC) times higher than for STIS.

Both cameras show numerous small-scale features in the background which are related to the flat fields. These vary in size and have maximum strengths of about 12% in the WFC, and ~30% in the HRC.

Based on these results, we feel it would not be prudent to further decrease the bright Earth avoidance angle for ACS below the present value of 20°. It is conceivable, however, that a filter-dependent avoidance angle might have some merit, where UV and narrow-band observations are allowed at somewhat smaller avoidance angles.

References

Shaw, D., Reinhart, M., and Wilson, J., 1997, “Scattered Light from the Earth Limb Measured with the STIS CCD,” STIS Instrument Science Report 98-21.